7

Climate Change Impacts on Atmospheric Circulation and Daily Precipitation in the Argentine Pampas Region

Olga C. Penalba[1] and María Laura Bettolli[1,2]
[1]*Departamento de Ciencias de la Atmósfera y los Océanos, FCEN, UBA*
[2]*Consejo Nacional de Investigaciones Científicas y Técnicas*
Argentina

1. Introduction

The relevant findings of the Intergovernmental Panel on Climate Change (IPCC, 2007) highlight the increment of the global mean temperature and the need to understand how this increment will affect the climate variability and change of the regional environment. The changes in the climate are a consequence of both internal variability of the climate system and external factors, the latter being both natural and anthropogenic. The Fourth Assessment Report of IPCC describes the scientific progresses that have been achieved by researchers in the understanding the observed changes of the climatic system, the processes involved, and the establishment of future climate change projections (IPCC, 2007). The number of studies that discuss this problematic have increased considerable during the last years. However, there are many issues that need further investigation, in particular for developing countries.

Extreme climate anomalies have a negative impact on the population and economy of the affected regions. The climate has a fundamental role for regions where the economy is based on agriculture. The process of growing crops can be seriously affected by extreme temperatures, and the precipitation can be a limiting factor which conditions the success or failure of the production.

The region of interest in this study is the Pampas region, which comprises the most productive agricultural lands of Argentina. The most important grains of the country, like soybean, corn, wheat and sunflower are grown in this region. Together with their by-products, these crops promote the social and productive system of the region, and are one of the principal sources of fiscal incomes. In the campaign of 2008/09, more than 24 million hectares, compared to of the country's total of 28 million cultivated hectares of these grains, corresponded to the Pampas region (http://www.sagpya.mecon.gov.ar/). This region, located in the center east of Argentina, southeastern South America, have an extension of more than 600.000 km2. Since the grains are cultivated extensively without artificial irrigation, the precipitation is one of the climatic variables of main influence for the production, and is also a condition for the management of the crops. Therefore, the spatial and temporal distributions of the precipitation in the region, and its surplus or deficit, are of extreme importance for the successful harvests.

From the 1960s, the Pampas region was favored by an increase of precipitation on both the annual and seasonal scales (Fernández et al., 2006; Liebmann et al., 2004). This increase showed a non-stationary variability (Penalba &Vargas, 2004). Depending on the region and the time of the year, the observed cycles were: inter-decadal variability, trends, jumps or discontinuities (Barros et al., 2008; Boulanger et al., 2005; Penalba & Vargas, 2008). This hydrological condition displaced the agricultural border with around 200 km to the west, which favored substantially the agricultural activity, especially in the semiarid subregions.

However, these inter-decadal and inter-annual variations were observed in the extreme precipitation, on an annual scale and during the months of maximum precipitation (Penalba & Vargas, 2008). On a daily scale, the frequency of rainy days and of days of extreme precipitation, showed the same temporal variability (Penalba & Robledo, 2010). Furthermore, the temporal variability was greater, increasing the risk of droughts and their consequent negative impacts (Penalba et al., 2010). During 2008 and during almost the entire 2009, a severe rainfall deficit occurred in the region (Bidegain et.al., 2010), impacting strongly the gross domestic product. In Entre Ríos, which is a province within the Pampas region, the producers lost more than 50 millions of dollars in the corn harvest (Riani, 2009).

Rainfall events depend on, among other factors, the large-scale atmospheric fields. Therefore, the study of these circulation structures, their frequency, distribution and temporal variability are important elements for diagnosis and forecast, particularly in the context of future climate change.

Global Circulation Models (GCMs) are fundamental tools for climate change studies. Various studies shows that the GCMs have good capacity of representing characteristics of the South American circulation climatology, on temporal scales from monthly to decadal (Di Luca et al., 2006; Solman & Le Treut, 2006; Solman & Pessacg, 2006). On the other hand, the intermodel variability in the representation of monthly and seasonal characteristics of the precipitation and temperature in different regions of South America is high (Gulizia et al., 2009; Marengo et al., 2010; Rusticucci et al., 2010; Silvestri & Vera, 2008; Vera et al., 2006).

The skill of the GCMs in representing the circulation that conducts or conditions the precipitation events has an important role in the evaluation of future climate projections. However, the capacity of the GCMs in representing the circulation on a synoptic scale has been little explored up to now. The usefulness of the GCMs in local studies is restricted by their poor spatial resolution. Techniques of scale reduction have been developed as bridges between the large scale information generated by the GCMs and the local scale information, with the purpose of performing short- to midrange forecasts and to study the potential impacts of future climate change. In this way, the use of daily results from the GCMs for studies of local climate is subject to their aptitude in representing the atmospheric systems on a regional scale.

In this context, the present chapter is structured to fulfill the following objectives: to characterize the rainfall conditions and their probability of occurrence in the Pampas region; to identify daily circulation patterns in southern South America and to associate them with different rainfall conditions in the Pampas region; to evaluate the representation of the daily circulation patterns as simulated by a set of 12 GCMs; and to analyze the projected changes of the same patterns at different time horizons of the 21th century.

In the second section of this chapter, the area, data and methods of this study are described. In the third section, the results are analyzed and discussed and in the last section the conclusions are presented.

2. Data and methods

2.1 Data

The following data-sets were used in this study:

a. Daily mean sea level pressure (SLP) fields from NCEP reanalysis 2, provided by the NOAA/OAR/ESRL PSD, Boulder, Colorado, USA: http://www.cdc.noaa.gov/, were used to represent observed circulation for the period 1979-1999. The domain extends from 15ºS to 60ºS and from 42.5ºW to 90ºW on a 2.5º latitude-longitude grid, including the Pacific and the Atlantic Oceans and the Andes Mountains, geographical features that have a significant influence on the circulation over South America (Figure 1).

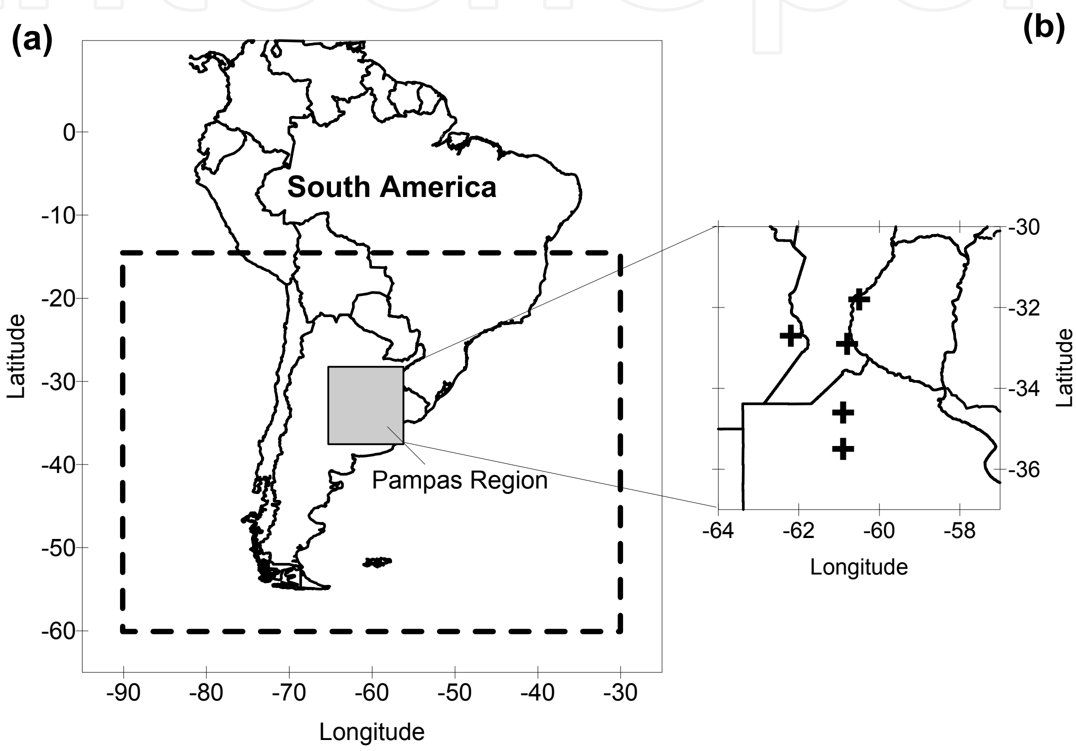

Fig. 1. (a) The Argentine Pampas Region (shaded rectangle) and the domain chosen for the atmospheric circulation fields (dashed line). (b) Locations of the five meteorological stations used in this chapter.

The focus of this analysis is to examine the model veracity with respect to sea level pressure. Previous studies (e.g. Bettolli et al., 2010) observed that the upper level patterns are less variable than the surface patterns. Furthermore, the upper level patterns can be associated with different surface synoptic types. The surface fields with their embedded synoptic systems provide a first-order control on spatial and temporal variations in precipitation.

b. Observed daily rainfall series from stations in the Pampas region were provided by the Argentine National Meteorological Service. The five stations that had both less than ten per cent of missing data and a continuity of their records were chosen for analysis (Figure 1) Although this dataset goes further back in time, we only analyze the period that coincide with the NCEP data period.

c. A set of 12 GCM SLP daily fields was used to describe present and future low level circulation (Table 1). The 20C3M experiment was used for the period 1979-1999 and the

SRES A1B 720 ppm stabilization scenario was used for the periods 2046-2065 and 2081-2099. These simulations are available from the Program for Climate Model Diagnosis and Intercomparison (PCDMI) and from the ENSEMBLES CERA archives.

The SLP fields of the models were interpolated to the NCEP reanalysis grid with an inverse distance weighting method in order to facilitate comparisons.

Identification	Model	Original Grid Resolution
A	BCCR-BCM2.0	2.7905° x2.8125 °
B	CNRM-CM3	2.79° x 2.8125°
C	CSIRO-Mk3.0	1.865° x 1.8750°
D	ECHAM5/MPI-OM	1.865° x 1.8750°
E	EGMAM	3.71059° x 3.75°
F	GFDL-CM2.0	2° x 2.5°
G	GFDL-CM2.1	2° x 2.5°
H	GISS-EH	3° x 5°
I	GISS-ER	3° x 5°
J	INGV-SXG	1.1215° x 1.125°
K	IPSL-CM4	2.5352° x 3.75°
L	UKMO-HadCM3*	2.5° x 3.75°

* Available period for present climate: 1979-1989

Table 1. List of GCMs used for the study.

2.2 Methods

In order to identify the dominant spatial structures and their degree of contribution to the total variance, Principal Component Analysis (PCA) was performed on observed NCEP SLP field (Jolliffe, 2002; Richman, 1986). The method was applied in the T-mode, withthe correlation matrix as input and the SLP daily fields as variables and the gridpoints as observations. Only the principal components (PCs) that correspond to large eigenvalues are expected to contain an interpretable signal and are retained for further analysis. Craddock & Flood (1969) suggest plotting the log eigenvalue diagram (LEV diagram) and cutting the number of PCs just behind a section where the graph approximates to a line with a relatively small slope. Following their criterion, the first 6 PCs for summer and the first 8 PCs for winter, accounting for 94.3% and 94.6% of the total variance respectively, were retained for further analyses. The first unrotated PC of the raw data can be identified with the time mean pattern (Compagnucci & Vargas, 1986; Huth, 2000). The first PC was calculated for each GCM in order to analyze the ability of the GCMs to reproduce the basic characteristics of the daily circulation at low levels.

The cluster analysis was coupled with PCA to determine the dominant circulation types (CT) of NCEP (as in Romero et al., 1999a; Rodrigues Chaves & Cavalcanti, 2001). The analysis was carried out in the subspace given by the leading unrotated PCs. As shown by Gong & Richman (1995), this combination of methods provides the most separable cluster system. The clustering algorithm used in this study is the ‘k-means’ method, which is a partitioning method that classifies all days into a predefined, optimal number of clusters (MacQueen, 1967). The method minimizes the variability within each cluster and maximizes the variability between clusters.

The choice of optimal number of clusters was established by the pseudo-F statistic (Calinski & Harabasz, 1974). This statistics assess the among- and within-cluster sum of squares relationship. The number of maximum local peaks in its plot indicates an appropriate number of clusters (Romero et al., 1999b). A progressive number of k clusters, from 2 to 30 were tested, and the pseudo-F statistic suggested a five-cluster solution for summer and a seven-cluster solution for winter.

The SLP fields from the GCMs, were classified using the cluster centroids from the NCEP original typing. Each GCM SLP daily field was assigned to the NCEP circulation type that correlated best with the daily field.

In order to outline and summarize the model-data comparisons, Taylor diagrams were constructed (Gleckler et al., 2008). These diagrams convey information with clarity and they quantify the degree of statistical similarity between two fields (in this study, between the observed NCEP circulation and the simulated by the GCMs) considering the correlation coefficient, the standard deviation and the root mean squared error (RMSE). The shape of the configurations can be compared, to a certain degree, through the correlation coefficient. The spatial patterns are compared directly from the values of atmospheric pressure through the standard deviation and the RMSE. The GCMs are considered to characterize and estimate the spatial patterns better, when the cloud of points is more concentrated and closer to the reference point.

The probability of occurrence of a given rainfall event conditioned to a specific circulation type (CT) was compared to the climatological probability of its occurrence (Bettolli et al., 2010). The Z statistic was used to quantify the difference between the probabilities (Infante Gil & Zárate de Lara, 1984).

3. Results

3.1 Precipitation

The Pampas region has a humid temperate climate and a flat relief. The mean annual rainfall is around 900 mm. The annual rainfall is characterized by a spatial variation in the NE-SW direction, with a significant decrease from east to west from the meridian of 65° (Penalba & Vargas, 2008). Of the annual amount, only 20% reaches the sea as water and the remaining 80% evaporates, runs off or changes the soil water amount (Berbery & Mechoso, 2001). The mean annual cycle of the region is characterized by a wet season with around 110 mm per month from October to April (warm months). During the transition months, the monthly rainfall decreases, reaching its lowest values during austral winter (around 30 mm/month) (Bettolli et. al., 2010).

In some recent application studies, the number of rain days appeared to be the key to fluctuations in total rainfall amounts; in some, variation depended on rainfall intensity; and in others, on both variables. It has also been found that the lack of water can affect crop production.

Robledo & Penalba (2008) analyzed the climatology of the different components that affect the monthly rainfall of Argentina. They calculated the amount and the frequency of the mean daily intensity and the daily extreme rainfall, using different thresholds according to the regions. In the Pampas, the spatial patterns and seasonal variation of daily rainfall above the 75^{th} percentile show similar behavior. From October to April, the value of this threshold is around 16 mm/day, meanwhile during winter this value decreases to 5 mm/day. The frequency of rain days during the wet months is around 25%, decreasing to 16% during the austral winter months.

Considering the dry condition, the average length of a dry sequence is 5 days or 8 days in summer and winter, respectively. The maximum dry period length presents more spatial variability with values around 20 days in summer and 40 days in winter (Llano & Penalba, 2011).

In this chapter, we are interested in the characteristics of the rainfall that condition the production of crops. Winter and summer coincide with key stages of the growing season of main crops of the region (Pascale & Damario, 2003). Dry or wet conditions are defined at a regional scale, analyzing the joint information of the five stations. We analyze days with no rainfall in the five stations of the region (dry days), days with rainfalls in at least one station in the region greater than 0.1mm (rain days, R0.1) and greater than the 75th percentile (heavy rain days). As mentioned above, the 75th percentile for winter is 5mm (R5) and 16mm (R16) for summer.

The annual cycle of the percentage of days corresponding to different rainfall conditions is shown in Figure 2. The annual cycle pattern of the three humid conditions is conserved in the region, with low variability on a monthly time scale for both winter and summer seasons. The highest variability between the months of these seasons is found in the R0.1 condition. During summer, in general, the probability of rainfall at least at one station is around 50% and of intense rainfall 20%. For winter, these probabilities are 30% and 10% respectively. Although the region is classified as humid, due to its high annual precipitation amount, the annual percentage of dry days is more than 50 per cent.

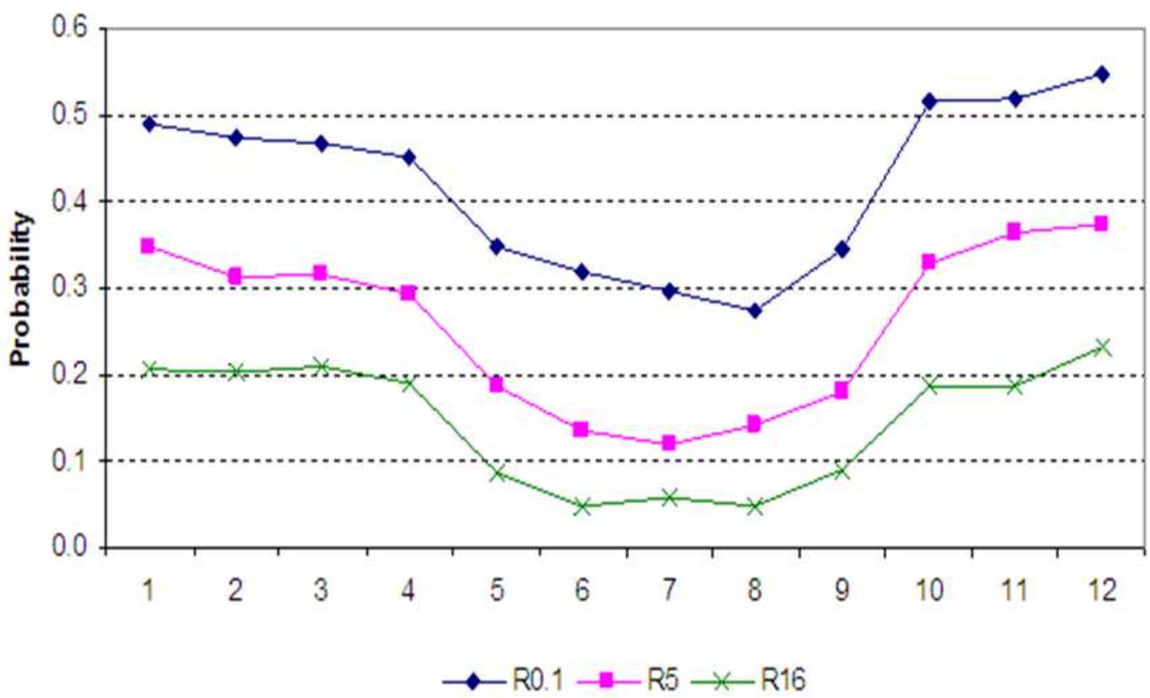

Fig. 2. Annual cycle of the probability of days per months corresponding to different rainfall conditions: 0.1 mm (R0.1), 5mm (R5), 16mm (R16) in at least one station in the region.

The daily rainfall of 10mm plays an important role for the hydrological balance of the summer months, since this amount approximates the daily evaporation (R10) (Vargas, 1979). Due to the hydrological characteristics of the Pampas region, the analysis focus on winter (JJA) and summer (DJF), coinciding with key stages of the growing season of different main crops in the region (wheat, corn and soybean). The thresholds of study are set 1 to R0.1 and no rain for both seasons and to R5 for winter and to R10 and R16 for summer.

3.2 Climatic characteristics of the atmospheric circulation

One important aspect when comparing the properties of the GCMs and NCEP dataset is the reproduction of the PCs spatial structures. In particular, the first PC spatial pattern approximates the time mean pattern; whereas the remaining PCs spatial patterns can be interpreted as deviations from the time mean (Huth, 2000). This feature is used to analyze the climatology of the GCMs.

The climatic characteristics of the mean SLP patterns, represented by the first PC of NCEP datasets, show a notorious seasonality (Figure 3). This seasonality is of great importance in determining the low-level circulation and its associated moisture advection to the region. During summer, the high pressure cells over the eastern South Pacific and western South Atlantic are positioned in their southernmost location, limitating the Westerlies to the south of 50ºS. A clear thermo-orographic low is located in the center of the continent over the eastern Andes mountain range. During winter, both the semi-permanent high systems and the Westerlies are in their northernmost position and the thermo-orographic low is absent. These climatic characteristics seem to be better captured by the GCMs in winter than in summer (Figure 3). The scatter plot diagrams of Figure 3 show that the cloud of points is more concentrated and closer to the point of high correlation (between the spatial patterns of the PC1 of NCEP and of the models), and lesser RMSE.

The spatial patterns of the best and worst performing GCMs, that is, the GCMs located at the extreme points of the scatter plot diagrams, are also shown in Figure 3. During winter, the GCMs tend to displace the Westerlies equatorward, attenuating the contribution of the subtropical highs, whereas in summer, both semi-permanent high systems are more extended to the south. For some GCMs, the difficulty in representing the Andes orographic effect on the circulation is noteworthy. As examples, the model GISS-ER and EGMAM are shown in Figure 3. GISS-ER extends the thermo-orographic low of summer towards a larger region over the mountain range, while the model EGMAM represents both semi permanent anticyclones over the continent, penetrating the range.

The variance explained by each PC can be interpreted as a measure of the strength of each spatial pattern. Therefore, an analysis of the variance values explained by the first PC is used as a simple indicator of the ability of the GCMs in representing the mean fields of the low level circulation over the region. The percentages of variance explained by the first PC are shown in Figure 4. For the NCEP dataset, values reach 70.6% and 54.6% for summer and winter respectively, indicating that the cold season is more perturbed than the warm season. During summer, the percentage of variance explained by the first PC of 10 out of the 12 GCMs is below than observed. Thus, most models tend to represent a lesser incidence of the mean pattern and, therefore, a higher presence of perturbations. During winter, 6 models keep the circulation closer to its mean than is observed (i.e., overestimation in the percentages of variance explained by the first PC in BCCR-CM2.0, CNRM-CM3, CSIROMk3.0, GFDL-CM2.0, UKMO-HadCM3 and IPSL-CM4). However, the inter-model dispersion is lower when compared with summer. It is worth mentioning that most models are capable of reproducing the seasonality of the percentage of variance explained by the first PC, which is lower in winter. The exception is IPSL-CM4 with a lower percentage in summer.

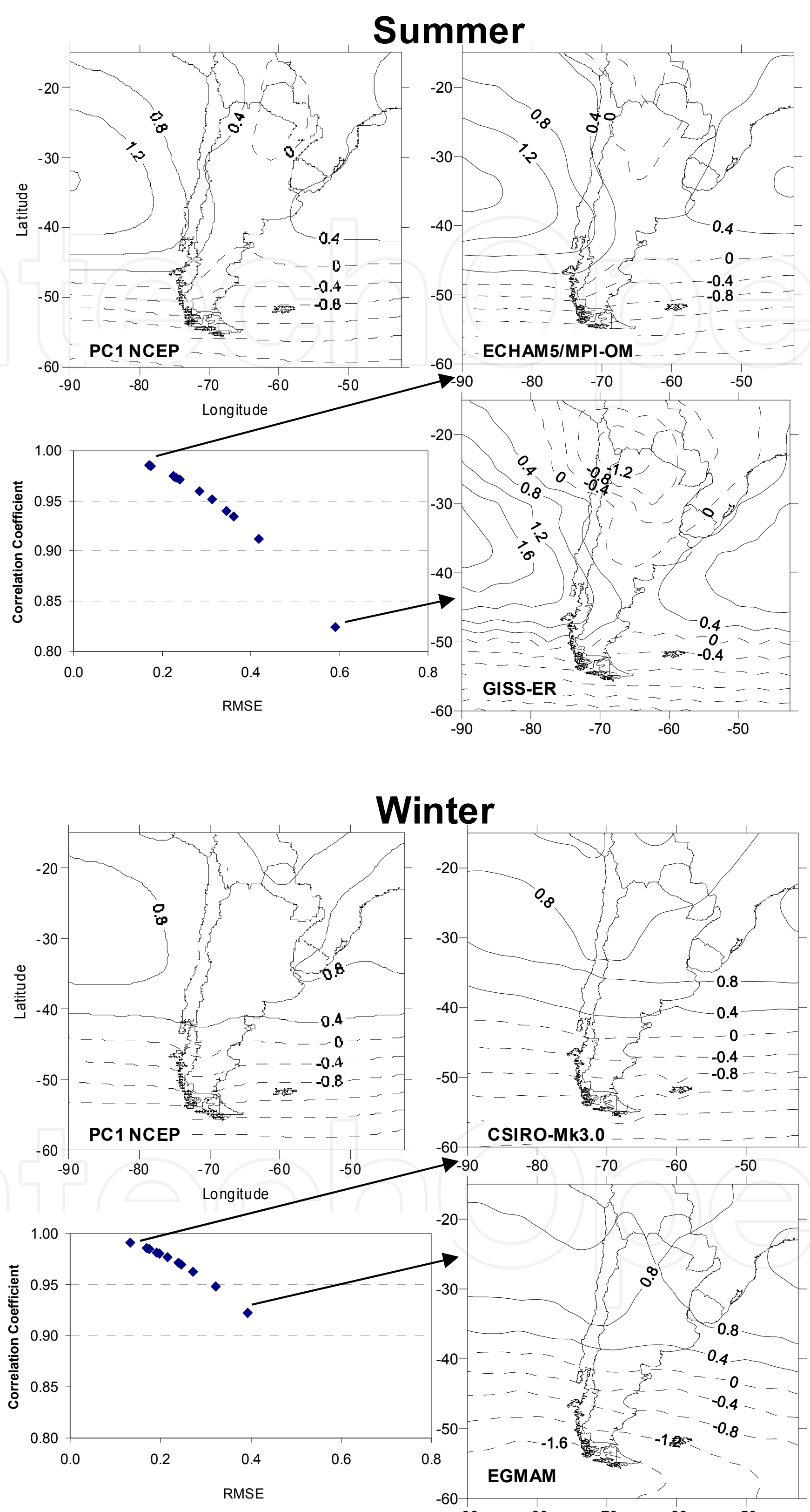

Fig. 3. Spatial pattern of the PC1 of the NCEP SLP data for summer and winter. Scatterplot of the correlation coefficients versus the RMSEs between PC1 of NCEP and of the GCMs. Spatial pattern for some selected models are also shown.

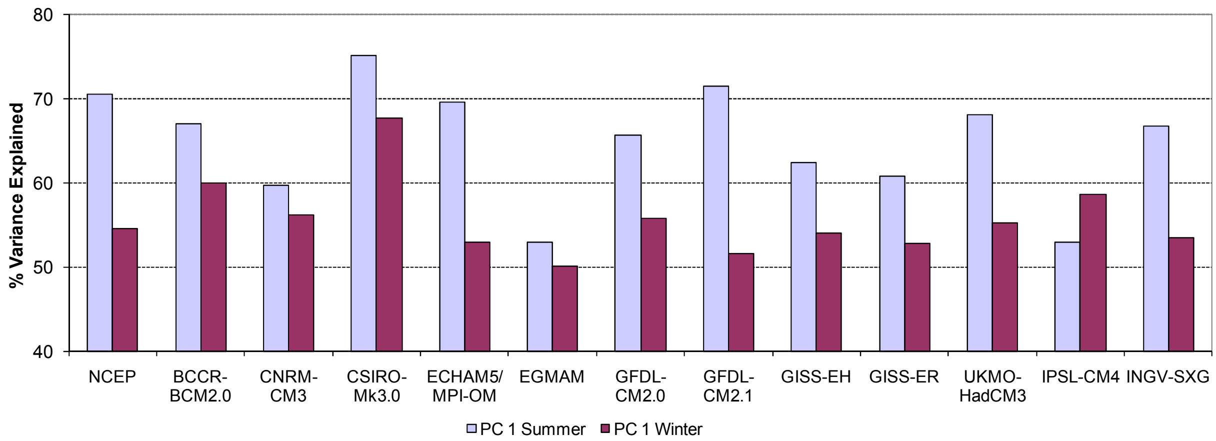

Fig. 4. Percentage of variance explained by the PC1 for summer and winter.

3.3 Observed circulation types

The circulation types for summer (CTi_S, i=1,…,5) are shown in Figure 5.

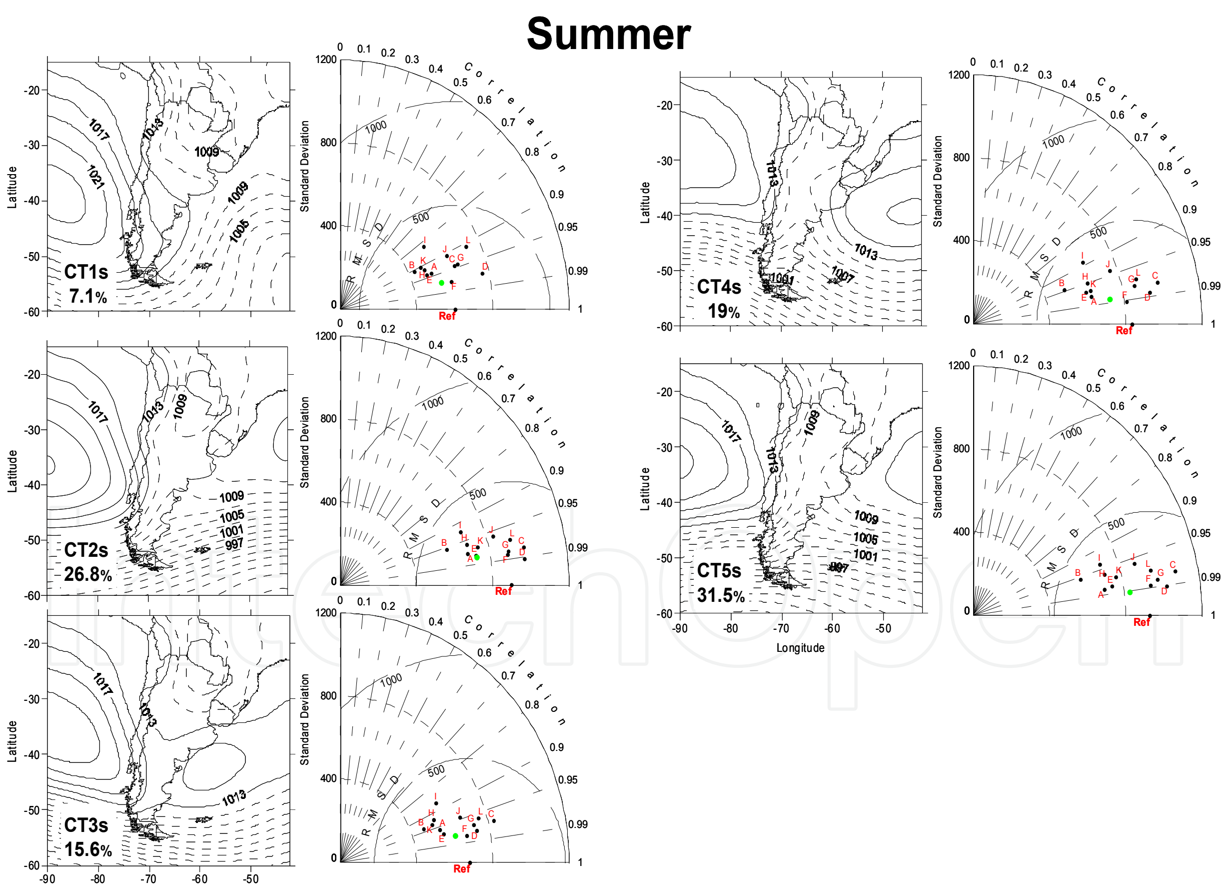

Fig. 5. Observed CTs and percentage of days corresponding to each CT for summer. The dashed (solid) lines represent sea level pressure values lower (higher) than 1013 hPa. The contour interval is 2 hPa. Taylor diagrams of the observed CTs of NCEP and the CTs of the GCMs (red letters) and of the model ensemble (green point).

$CT1_S$ is characterized by an intensification of the southern Pacific anticyclone associated with a trough axis in the northwest-southeast direction. This structure could be connected with a post-frontal anticyclone that moves forward on the continent inducing an anomalous flow from the east-southeast over the Pampas region. $CT2_S$ is characterized by a perturbation over the continent and a weakening of the Atlantic anticyclone that could be related to a cold front affecting the region. In $CT3_S$, a belt of high pressures is extended to the South, reaching around 45ºS. This CT is accompanied by a centre of low pressure values to the north. $CT4_S$ shows an intensification and expansion of the southern Atlantic anticyclone, which interrupts the passage of the eastern perturbations and diverts them to the south. $CT5_S$ is the pattern that is most similar to the mean SLP field of summer (compare with the spatial pattern of the NCEP PC1 in Figure 3). This is the most frequent summer pattern, with 31.5% of the studied cases.

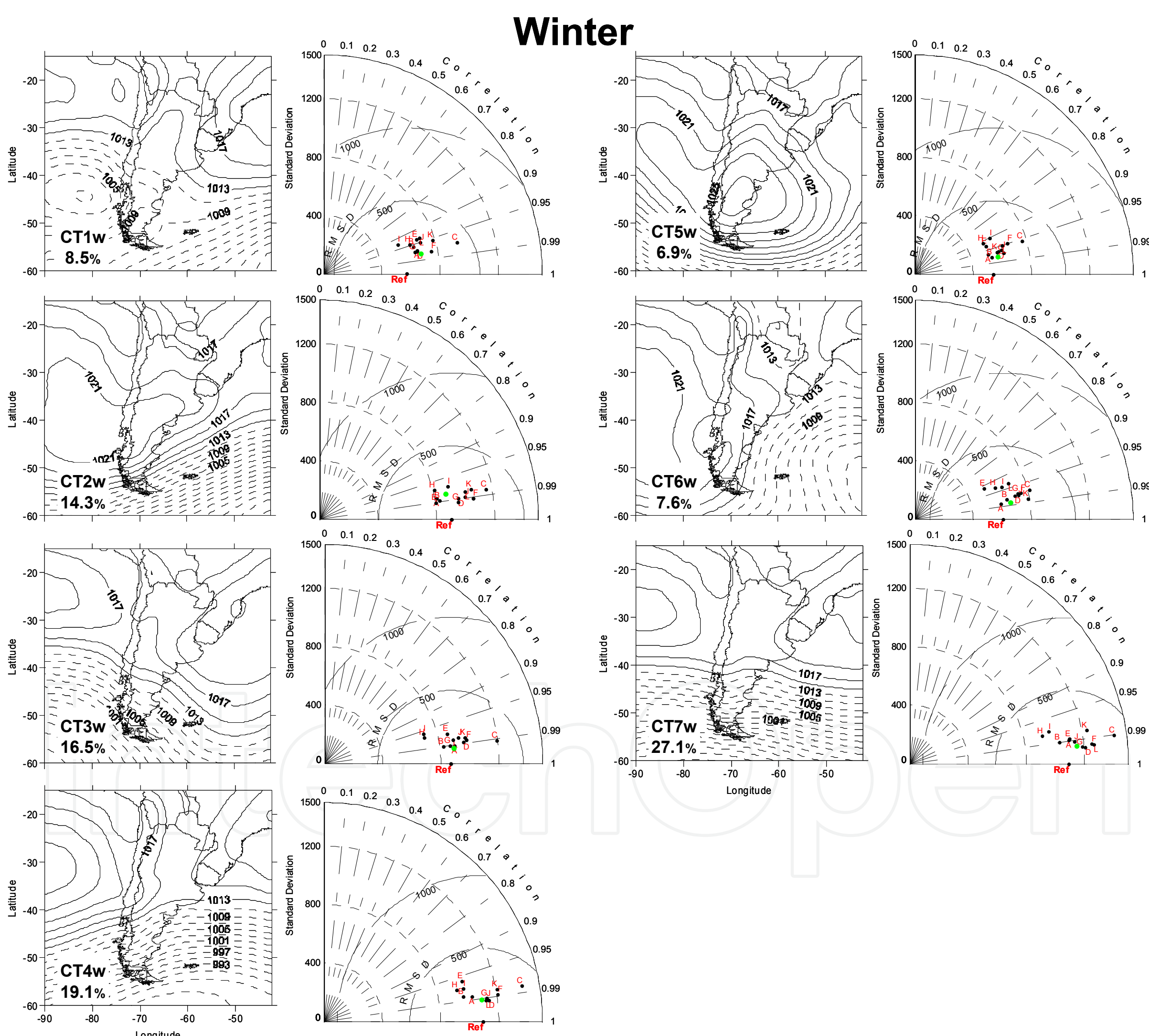

Fig. 6. Idem Figure 5 for winter.

The winter patterns (CTi_W, i=1,…,7) show more variable spatial structures than the summer patterns (Figure 6). This is due to the higher baroclinicity of the winter season and therefore, the greater contribution of synoptic perturbations. In $CT1_W$, a cyclonic perturbation dominates the circulation over the southern South Pacific Ocean, while the opposite occurs in $CT2_W$ for which a high pressure system extends towards south, entering over the continent. $CT3_W$ shows an intensification of the Atlantic anticyclone, inducing an anomaly of the northern-northeastern flow at the southern tip of the continent. $CT3_W$ shows an extension towards the north of the Westerlies, which restricts the action of both anticyclones to act to the north of 40ºS. $CT5_W$ corresponds to an intense high pressure centered over Patagonia in the south of Argentina that extends over almost the whole southern region of the continent and over adjacent oceans. $CT6_W$ can be associated with a cold front that advances towards northeast with its postfrontal anticyclone generating southern advection when getting in over the continent. Finally, $CT7_W$ can be linked with the mean SLP field of winter, similarly to summer, with a frequency of 27.1% (compare with the spatial pattern of the NCEP PC1 in Figure 3).

3.4 Observed circulation types and daily rainfall

This section quantifies the relationship between the CTs for each season and rainfall amount and persistence over the Pampas region. The purpose is to evaluate how much rainfall information for the core crop-producing region is contained in the circulation structures at a regional scale. Then, the probability of occurrence of a rainy day conditioned to a specific CT is compared with the probability of occurrence of a rainy day for the rest of the data by means of the Z-statistic. Values and significance from the Z-statistics are shown in Table 2.

Summer				
	Dry Days	**R0.1**	**R10**	**R16**
CT1s	**-2.65**	**2.65**	-0.06	-1.13
CT2s	**-2.22**	**2.22**	**2.25**	**2.29**
CT3s	0.67	-0.67	-0.99	-1.51
CT4s	**3.68**	**-3.68**	**-3.05**	**-2.16**
CT5s	-0.05	0.05	1.00	1.15

Winter			
	Dry Days	**R0.1**	**R5**
CT1w	-1.20	1.20	0.75
CT2w	1.21	-1.21	**-2.26**
CT3w	0.33	-0.33	-0.71
CT4w	**1.78***	**-1.78***	-1.36
CT5w	**-4.72**	**4.72**	**3.06**
CT6w	-1.56	1.56	0.44
CT7w	**1.99**	**-1.99**	0.34

Table 2. Z-statistics of the comparison between the conditional probability of occurrence of a day with a certain rainfall condition in each CT for summer and winter and the climatological probability of that day. If the Z-statistic value is positive (negative) and is significant, the specific circulation pattern has (does not have) a significant contribution to the rainfall event. In red, significant values at 95% and 90% (*).

For summer, $CT4_S$ has the highest contribution to the dry days, showing positive and significant values of the Z-statistic for this condition (first column in Table 2). The configuration of SLP of $CT4_S$ corresponds to an intensification of the southern Atlantic anticyclone, which interrupts the passage of the eastern perturbations and diverts them to the south. This anticyclone induces stability at low levels and can be significantly associated to the dry days of the region. $CT4_S$ is the most persistent pattern, with the 19% of the events in sequences lasting from four to seven-day (Table 3). For rainy days, positive and significant values of the Z-statistic are observed for the $CT2_S$ and $CT1_S$ patterns (R0.1, R10 and R16 columns in Table 2). Rainy days (R0.1) are significantly benefited by patterns that could be related to a post-frontal intense anticyclone that induces east-southeast anomalous flow and consequently increases moisture advection over the region (CT1s). This pattern is the less frequent NCEP pattern of the season (7.1%, Figure 5) and is also one of the less persistent patterns, with 90% of the events in sequences of one to three days (Table 3). Heavy rainy days are significantly related with a cyclonic disturbance at the centre of the continent associated with a cold front passage ($CT2_S$ in Figure 5).

	Summer					Winter						
D	**CT1s**	**CT2s**	**CT3s**	**CT4s**	**CT5s**	**CT1w**	**CT2w**	**CT3w**	**CT4w**	**CT5w**	**CT6w**	**CT7w**
1	54.3	41.1	60.5	34.8	46.7	36.6	50.3	36.8	52.5	59.5	51.3	48.3
2	24.3	23.7	22.2	31.2	22.2	33.8	25.5	27.8	20.1	21.5	30.0	24.6
3	11.4	17.8	9.0	12.1	12.8	11.3	14.5	16.5	12.3	12.7	6.3	12.7
4	4.3	8.7	4.8	8.5	7.4	7.0	5.5	9.0	7.3	2.5	10.0	3.8
5	1.4	3.2	0.6	4.3	4.7	5.6	2.1	5.3	2.8	3.8	2.5	5.5
6		2.7	0.0	4.3	1.9	2.8	1.4	1.5	2.8			0.8
7	4.3	0.9	2.4	2.1	0.8	1.4	0.0	0.0	1.1			1.7
8		1.4		1.4	1.6	1.4	0.7	2.3	1.1			0.4
9			0.6	0.7	1.2							0.8
10												0.4
11		0.5		0.7	0.4							0.4
12												
13					0.4							
14												
15												0.4

Table 3. Probability of the persistence (in days, D) of the different CTs.

Summer		Winter	
CT1s	Rainy Days Least Frequent	**CT1w**	
CT2s	Heavy Rainy Days	**CT2w**	
CT3s	Least persistent	**CT3w**	Most persistent
CT4s	Dry Days Most persistent	**CT4w**	Dry Days
CT5s	Most frequent	**CT5w**	Rainy and heavy rainy Days Least persistent Least frequent
		CT6w	Rainy Days
		CT7w	Dry Days Most frequent

Table 4. Schematic summary of results.

In Table 4, a schematic summary of the results described above is found, which will serve as a basis for the comparison with the GCMs in the next section.

Winter dry days are significantly favored by a high pressure system that extends from the Atlantic Ocean to the centre of the continent ($CT4_W$) and also by $CT7_W$, the pattern that resembles the mean pattern for winter (positive and significant values of the Z-statistic for this condition in the first column of Table 2). Rainy days and heavy rainy days are significantly benefited by structures with a high pressure system at the south of the continent, enhancing an anomalous flow from the east-southeast to the central region of Argentina and a corresponding moisture advection at low levels ($CT5_W$). This CT is the less persistent pattern with 93.7% of the events in sequences of one- to three-day lasting (Table3) and it is also the less frequent one (6.9%, Figure 6). $CT3_W$ is the most persistent pattern of winter (Table 3), coinciding with what was found for the summer $CT4_S$.

3.5 Comparison between NCEP and GCMs

3.5.1 Present climate

A diversity of aspects should be taken into account when comparing the ability of the GCMs in representing the synoptic patterns of NCEP, given that the surface climate depends on the representation of these characteristics.

The comparison of the mean spatial patterns is summarized in the Taylor diagrams of Figures 5 and 6. Although the correlation is expected to be high, since the projection of the GCM fields was defined over the centriods of the observed NCEP fields, a certain dispersion is found.

In summer, $CT2_S$ and $CT5_S$ shows the smallest dispersion, bounded between the values 0.95 and 0.99 of the Taylor diagrams. This means that the GCMs are able to reproduce the structure and position of these atmospheric systems. In particular, the accurate representation of $CT2_S$ is essential for the generation of the heavy rainfall events in the region.

In winter, the greatest correlations are close to 0.99 and are found for the $CT2_W$, $CT3_W$, $CT4_W$ and $CT7_W$. Unlike what occurs for summer, the CTs that are best represented by the GCMs are the ones associated with dry days ($CT4_W$ y CT7w). CT3w is the most persistent structure with an intensification of the Atlantic anticyclone (Table 3) that could be linked to the blocking events occurring in the Atlantic ocean (around 40°W) that are more frequent during winter (Alessandro, 2003). From the Taylor diagram, it is clear that the spatial structure of CT3w is well represented, which is key for the location of the blocking and its consequent effect on the surface variables (Figure 6).

The comparison of the standard deviation and the root mean squared error indicate an inter model dispersion according to the CT and the time of the year. For summer, the standard deviations are distributed around the observed NCEP value for all cases except for CT2s, for which most models underestimate the standard deviation (points to the left of the reference point in the Taylor diagram of Figure 5). This indicates that the GCMs tend to underestimate the amplitude of the variation of the SLP of CT2s, and consequently underestimate the depth of the systems that are associated directly with heavy rainfall.

During winter, the dispersion of the standard deviations is uniform for $CT2_W$, $CT3_W$, $CT4_W$ y $CT7_W$, which also are the CTs with best estimations of the spatial structures (Figure 6). Most GCMs overestimate the standard deviation of the types $CT1_W$, $CT5_W$ and $CT6_W$,

increasing the depth of the systems, and in particular of those that are associated with rainfall or heavy rainfall of winter ($CT5_W$ and $CT6_W$, Table 4).
In all cases, the root mean squared errors are lower than 400 hPa. Considering that the standard deviations of NCEP vary between 536 and 1088 hPa, the model errors are lower than the proper variability of the observed mean fields. Also, the majority of the errors do not reach higher values than 50% of the standard deviation.
Another aspect to take into account is the relative frequency of each CT estimated by the GCMs. Figure 7.a shows that the ensemble is able to reproduce these frequencies, although the model dispersion is considerable, especially in summer for CT3s and CT5s. In summer, the frequencies of the models overestimate the frequencies of CT3s while the frequencies of CT5s are mostly underestimated. The latter coincides with what was found in the analysis of the dominant summer pattern, PC1. CT5s is similar to the summer mean field and an underestimation of its frequencies implicates a higher contribution of the other CTs, representing the perturbations. The pattern that represents an intensification of the southern Atlantic anticyclone and its stability (CT4s) is the pattern that is best represented by the GCMs in terms of frequency. This pattern is significantly associated to the dry days of the region.
For winter, the dispersion among the models is lower than for summer. $CT5_W$ and $CT6_W$ are best represented with frequencies close to observed values. This implies that the models are capable of a quite good representation of the frequencies of the structures that are significantly associated with rain days and heavy rain days. The ensemble reproduces the observed frequencies very well in all cases.

3.5.2 Future climate

The future frequency changes of each CT show a considerable dispersion among the GCMs (Figures 7.b and 7.c), especially for the warm season. Nevertheless, the signs of the tendencies are equal for all CTs and for the two time horizons (2046-2065 and 2081-2099). It is important to point out that the future changes of the CT frequencies are smaller than the 20th century observed frequency dispersion (Figure 7). In this sense, it is difficult to quantify the uncertainty.
In the previous section, it was found that the $CT2_S$ and $CT4_S$ are significantly associated with heavy rainy days and dry days respectively (Table 4). In the projections of future CTs, the majority of the GCMs and the ensemble show an increment of $CT2_S$ frequencies and a decrease of the $CT4_S$ frequencies. This is interpreted as a trend of reduction of the dry day circulation patterns and in an increase of the frequencies of the patterns associated with rainfall of the region. These results coincides with other climate change results over the region that shows positive trends in the total seasonal precipitation and changes in the precipitation variability (Barros et al., 2005; Silvestri & Vera, 2008; Vera et al., 2006).
For winter, even if there is a slight dispersion in the frequencies of the future projections, this does not seem to indicate mayor changes in the frequencies of the patterns. The main changes are given by an increase of the frequencies of $CT2_W$ and $CT7_W$, and a decrease of $CT1_W$ and $CT3_W$.
These results would imply an increment in the variability of daily rainfall, especially during summer, and also a change in the distribution of rainfall over the Pampas region.

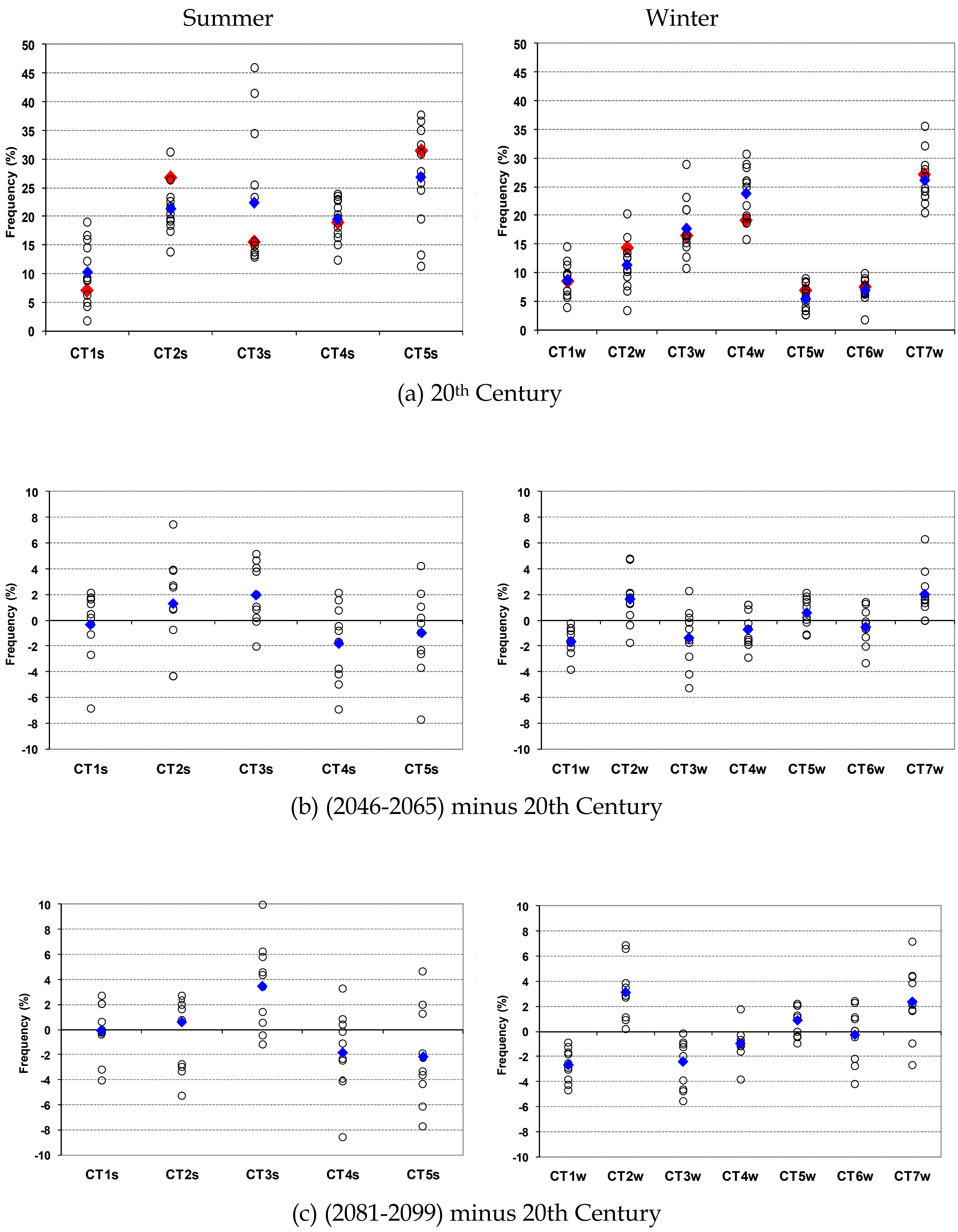

Fig. 7. Frequency (%) of circulation types for summer and winter for NCEP (red diamond), GCMs (circles) and ensemble of GCMs (blue diamond) for the 20th Century (a). Future changes of the frequencies of the CTs for the period 2046-2065 (b) and 2081-2099 (c).

4. Conclusion

This chapter analyzed the relation between the daily low level circulation over Southern South America and adjacent oceans and the precipitation over the region Pampas. Also, the capacity of 12 GCMs in representing the low level synoptic circulation for the period 1979-1999 was evaluated and their future projection of the XXI century was discussed.

The synoptic structures identified in this work can be associated with daily rainfall over the region of study. The classification scheme is effective not only in discriminating dry and rainy days, but also in differentiating between different thresholds of rainfall intensities. In this sense, the findings of this research help to improve our understanding of the relationship between rainfall variability and atmospheric circulation as defined by an objective classification of circulation types.

Summer dry days are related to the most persistent circulation type, corresponding to an intensification of the southern Atlantic anticyclone, which interrupts the passage of the eastern perturbations and diverts them to the south. Rainy days are significantly benefited by patterns that could be related to a post-frontal intense anticyclone that induces east-southeast anomalous flow and moisture advection over the region Heavy rainy days are significantly related with a cyclonic disturbance at the centre of the continent associated with a cold front passage.

Winter dry days are significantly favored by a high pressure system that extends from the Atlantic Ocean to the centre of the continent. Rainy days and heavy rainy days are significantly benefited by structures with a high pressure system at the south of the continent, enhancing an anomalous flow from the east-southeast to the central region of Argentina and a corresponding moisture advection at low levels.

The principal climatic characteristics of the atmospheric circulation of summer and winter are reasonably well captured by the GCMs, although the seasonality is exaggerated. For example, during winter, the Westerlies are displaced towards the equator, attenuating the contribution of the subtropical highs. During summer, both semi-permanent high systems more extended to the south than the observed fields. Most models tend to show a lower contribution of the mean pattern in comparison to NCEP and, therefore, a higher presence of perturbations.

With respect to the circulation types, the models are able to reproduce the full range of summer and winter circulation types found in the NCEP climatology. For present climate, an inter-model variability of the representation of the summer patterns is observed. The GCMs estimate reasonably well the frequency of atmospheric situations that favor dry days. For the two future time horizons analyzed, a trend of reduction of the circulation patterns associated with dry days and an increment of the frequencies of the patterns associated with rainfall of the region is observed. This is in agreement with other climate change studies over the region that shows positive trends in the total seasonal precipitation and changes in the precipitation variability.

Contrary to what is observed for summer, during winter the GCMs estimate reasonably well the frequency of the circulation types, especially those that favor heavy rain and dry conditions over the region. The majority of the GCMs indicate an increment of these patterns for future climate, principally during the second half of the 21^{th} century.

The results above imply an increment in the variability of daily rainfall, especially during summer, and also a change in the distribution of rainfall over the Pampas region. From

these projections, favorable consequences for the trends of the agricultural production in a climate change context can be derived, especially for the agricultural border.
However, it should be stressed that although the GCMs are capable of reproducing the circulation types and their main characteristics, there is an important intermodel dispersion. This limits the reliability of the GCMs for the study of future circulation changes, and consequently of precipitation changes. As explained above the quantification of the uncertainty of the projections is a complex issue. With this in mind, the findings of this research provide insight into the possible future climate change context.
One of the important aspects related to climate change, including climate variability, is the comprehension of extreme events and the skill of the models in representing their occurrence. The impact of climate adversities in agricultural activities makes it necessary to determine in what measure the spatial and temporal variability of climate is responsible for the yields of the crops and to generate tools that permit the supervision, the estimation of impacts and the design of alert systems. The world is facing a water crisis, but improved water management in rain-fed agriculture can build resilience to cope with future water related risks and uncertainties.

5. Acknowledgment

This work was supported by the grant X170 of the Universidad de Buenos Aires; and CLARIS LPB Project (European Community's Seventh Framework Programme under Grant Agreement No. 212492). Authors thank Pablo Krieger for his assistance in calculations and graphs.

6. References

Alessandro, A.P. (2003). Blocking action situations in the south of South America during the 1990s. *Meteorologica*, Vol. 28, No.1-2, pp 23-38, ISSN 0325-187X

Barros, V.R.; Doyle, M.E. & Camilloni, I.A. (2008). Precipitation trends in southeastern South America: Relationship with ENSO phases and with low-level circulation. *Theoretical and Applied Climatology*, Vol. 93, No. 1-2, (June 2008), pp. 19-33, ISSN 0177-798X

Barros, V.; Menéndez, A. & Nagy, G. (2005). *El cambio climático en el Río de la Plata*. Buenos Aires: Consejo Nacional de Investigaciones Científicas y Técnicas, ISBN 950-692-0664-4, Buenos Aires

Berbery, E. H. & Mechoso C.R. (2001), Climatology and Hydrology of the La Plata basin, Document of the VAMOS scientific study group on La Plata basin, http://meto.umd.edu/~berbery/lpb/laplata.html, 2001

Bettolli, M.L.; Penalba, O.C. & Vargas, W.M. (2010). Synoptic Weather Types in the South of South America and their Relationship to Daily Rainfall in the Core Production Region of Crops in Argentina. *Australian Meteorological and Oceanographic Journal*, 60, No. 1, (January 2010), pp. 37-48, ISSN 1836-716X

Bidegain, M.; Skansi, M.; Penalba, O. C.; Quintana, J. & Aceituno, P. (2010). Southern South America in "State of the Climate in 2009", *Bulletin of the American Meteorological Society,* 91, S150-S152

Boulanger, J.P.; Leloup, J.; Penalba, O.C.; Rusticucci, M.; Lafon, F. & Vargas, W.M. (2005). Observed precipitation in the Paraná-Plata hydrological basin: Long-term trends, extreme conditions and ENSO teleconnections. *Climate Dynamics,* Vol. 24, No. 4, (March 2005), pp. 393-413, ISSN 0930-7575

Calinski, R.B. & Harabasz, J. (1974). A dendrite method for cluster analysis. *Communications in Statistics.*, Vol. 3, No. 1, (January 1974), pp. 1-27, ISSN: 0361-0926

Compagnucci, R.H. & Vargas, W.M. (1986). Patterns of surface pressure field during July 1972-1983 in Southern South America and the Antarctic peninsula. *Proceedings of Third International Conference on Statistical Climatology*, Vienna, Austria, 23-27 June 1986

Craddock, J.M. & Flood, C.R. (1969). Eigenvectors for representing the 500 mb geopotential surface over the Northern Hemisphere. *Quaterly Journal of the Royal Meteorological Society*, Vol.95, No. 405, (July 1969), pp. 576-593, ISSN: 1477-870X

Di Luca, A.; Camilloni, I. & Barros, V. (2006). Sea-level pressure patterns in South America and the adjacent oceans in the IPCC-AR4 models, *Proceedings of 8th International Conference on Southern Hemisphere Meteorology and Oceanography*, ISBN 85-17-00023-4, Foz de Iguazú, Brasil, 24-28 April 2006

Fernández, A.; Ciappesoni, H. & Nuñez, M. (2006). Observed trends in precipitation and temperature over Argentina. *Proceedings of 8th International Conference on Southern Hemisphere Meteorology and Oceanography*, ISBN 85-17-00023-4, Foz de Iguazú, Brasil, 24-28 April 2006

Gleckler, P.J.; Taylor, K. E. & Doutriaux, C. (2008). Performance metrics for climate models. *Journal of Geophysical Research*, 113, D06104, doi:10.1029/2007JD008972, 2008

Gong, X. & Richman, M.B. (1995). On the application of cluster analysis to growing season precipitation data in North America east of the Rockies. *Journal of Climate,* Vol. 8, No. 4, (April 1995), pp. 897-931, ISSN 0894-8755

Gulizia, C.; Camilloni, I. & Doyle, M. (2009). Evaluation of the moisture transport and convergente in southern South America in the WCRP-CMIP3 multimodel dataset. MOCA-09, Montreal, Canada, 19-29 July 2009

Huth, R. (2000). A circulation classification scheme applicable in GCM studies. *Theoretical Applied Climatology,* Vol. 67, No. 1-2, (October 2000), pp. 1-18, ISSN: 0177-798X

Infante Gil, S. & Zárate de Lara, G. (1984). *Métodos Estadísticos*, Trillas, ISBN: 9682414229, México

IPCC (2007). Solomon, S., D. Qin, M. Manning, Z. Chen, M. Marquis, K.B. Averyt, M. Tignor and H.L. Miller (Eds.). (2007). *Climate Change 2007: The Physical Science Basis. Contribution of Working Group I to the Fourth Assessment Report of the Intergovernmental Panel on Climate Change*, Cambridge University Press, ISBN: 978 0521 70596-7, Cambridge, United Kingdom and New York, NY, USA

Jolliffe, I.T. (2002). *Principal Component Analysis*, Springer-Verlag, ISBN 978-0-387-95442-4, New York, USA

Liebmann, B.; Vera, C.; Carvalho, L.; Camilloni, I.; Hoerling, M.; Allured, D.; Barros, V.; Báez, J. & Bidegain, M. (2004). An observed trend central S. American precipitation. *Journal of Climate,* Vol. 17, No. 22, (November 2004), pp 4357-4367, ISSN 1520-0442

Llano, M.P. & Penalba O.C. (2011). A climatic analysis of dry sequences in Argentina. *Internacional Journal of Climatology* , Vol. 31, No. 4, (March 2011), pp 504-513, ISSN 0899-8418

MacQueen, J. (1967). Some methods for classification and analysis of multivariate observations. *Proceedings of Fifth Berkeley Symposium on Mathematical Statistics and Probability*. Berkeley CA, University of California Press, USA

Marengo, J.; Rusticucci, M.; Penalba, O. C. & Renom, M. (2010). An intercomparison of model-simulated in extreme rainfall and temperature events during the last half of the XX century. Part 2: Historical trends. *Climatic Change.* Vol. 98, No 3-4, (February 2010), pp. 509-529, ISSN 0165-0009

Pascale, J.Y. & Damario, E.A. (2004). *Bioclimatología agrícola y agroclimatología*, Universidad de Buenos Aires, ISBN 9789502908229, Buenos Aires, Argentina

Penalba, O.C.; Rivera, J. A. & Bettolli, M.L. (2010). Trends and periodicities in the annual amount of dry days over Argentina. Looking towards the climatic change. *Second International Conference on Drought Management: Economics of Drought and Drought Preparedness in CIHEAM Journal Options Méditerranéennes*, 4 – 6 March 2010, Istanbul, Turkey

Penalba, O. C. & Robledo, F. (2010). Spatial and temporal variability of the frequency of extreme daily rainfall regime in the La Plata Basin during the 20th century. *Climatic Change.* Vol. 98, No.3-4, (February 2010), pp 531-550, ISSN 0165-0009

Penalba, O.C. & Vargas, W. M. (2004). Interdecadal and Interannual variations of annual and extreme precipitation over central-northeastern Argentina. Changes in the extreme precipitation seasonal cycle. *International Journal of Climatology*, Vol. 24, No 12, (October 2004), pp. 1565-1580, ISSN 0899-8418

Penalba, O.C. & Vargas, W.M. (2008). Variability of low monthly rainfall in La Plata Basin. *Meteorological Applications,* Vol. 15, No. 3, (September 2008), pp. 313 – 323, ISSN 1469-8080

Riani, J. (2009). Importantes pérdidas por la sequía en Entre Ríos, La Nación, 22 May 2009.

Richman, M.B. (1986). Rotation of Principal Components. *International Journal of Climatology*, 6, pp. 293-335, ISSN 0899-8418

Robledo, F. & Penalba O.C. (2008). Análisis estacional de la frecuencia diaria y la intensidad de los eventos extremos de precipitación sobre el sudeste de Sudamérica, *Meteorologica*, Vol 32 (33), No 1-2, pp. 31-49, ISSN 0325-187X

Rodrigues Chaves, R. & Cavalcanti, I. (2001). Atmospheric Circulation Features Associated with Rainfall Variability over Southern Northeast Brazil. *Monthly Weather Review,* 129, No 10, (October 2001), pp. 2614-2626, ISSN 1520-0493

Romero, R.; Sumner, G.; Ramis, C. & Genovés, A. (1999a). A classification of the atmospheric circulation patterns producing significant daily rainfall in the Spanish Mediterranean area. *International Journal of Climatology*, Vol. 19, No. 7, (June 1999), pp. 765–785, ISSN 0899-8418

Romero, R.; Ramis, C.; Guijarro, J. & Sumner, G. (1999b). Daily rainfall affinity aeras in mediterranean Spain. *International Journal of Climatology*, Vol. 19, No. 5, (April 1999), pp. 557-578 ISSN 0899-8418

Rusticucci, M.; Margeno, J.; Penalba, O.C. & Renom, M. (2010). An intercomparison of model-simulated in extreme rainfall and temperature events during the last half of the XX century. Part 1: Mean values and variability. *Climatic Change,* Vol. 98, No. 3-4, (February 2010), pp. 493-508,. ISSN 0165-0009

Silvestri, G. & Vera, C. (2008). Evaluation of the WCRP-CMIP3 model simulations in the La Plata Basin. *Meteorological Application,* Vol. 15, No. 4, (December 2008), pp. 497–502, ISSN 1469-8080

Solman, S. & Le Treut, H. (2006). Climate change in terms of modes of atmospheric variability and circulation regimes over southern South America. *Climate. Dynamics*, Vol. 26, No. 7-8, (June 2006), pp. 835–854, ISSN 1432-0894

Solman, S. & Pessacg, N. (2006). Analysis of low frequency variability patterns and circulation regimes over southern South America and their response to global warming as depicted by IPCC AR4 AOGCMs. *Proceedings of 8th International Conference on Southern Hemisphere Meteorology and Oceanography*, Foz de Iguazú, Brasil, 24-28 April 2006

Vargas, W.M. (1979). *Atlas. Excesos y Déficits de Humedad en la Región Húmeda y Semiárida Argentina. Tomo 1*. Instituto Nacional de Ciencia y Técnica Hídricas, Buenos Aires, Centro de Investigaciones Biometeorológicas

Vera, C.; Silvestri, G.; Liebmann, B. & Gonzalez, P. (2006). Climate change scenarios for seasonal precipitation in South America from IPCC-AR4 models. *Geophysical Ressearch Letters*, 33, L13707 doi:10.1029/2006GL025759

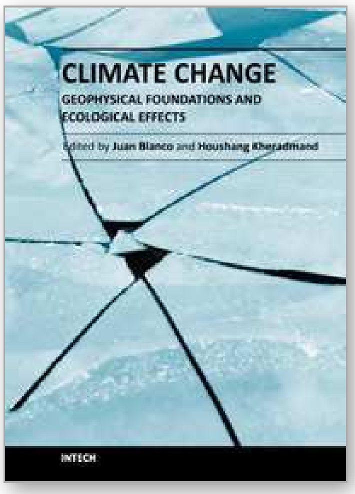

Climate Change - Geophysical Foundations and Ecological Effects
Edited by Dr Juan Blanco

ISBN 978-953-307-419-1
Hard cover, 520 pages
Publisher InTech
Published online 12, September, 2011
Published in print edition September, 2011

This book offers an interdisciplinary view of the biophysical issues related to climate change. Climate change is a phenomenon by which the long-term averages of weather events (i.e. temperature, precipitation, wind speed, etc.) that define the climate of a region are not constant but change over time. There have been a series of past periods of climatic change, registered in historical or paleoecological records. In the first section of this book, a series of state-of-the-art research projects explore the biophysical causes for climate change and the techniques currently being used and developed for its detection in several regions of the world. The second section of the book explores the effects that have been reported already on the flora and fauna in different ecosystems around the globe. Among them, the ecosystems and landscapes in arctic and alpine regions are expected to be among the most affected by the change in climate, as they will suffer the more intense changes. The final section of this book explores in detail those issues.

How to reference

In order to correctly reference this scholarly work, feel free to copy and paste the following:

Olga C. Penalba and Marîa Laura Bettolli (2011). Climate Change Impacts on Atmospheric Circulation and Daily Precipitation in the Argentine Pampas Region, Climate Change - Geophysical Foundations and Ecological Effects, Dr Juan Blanco (Ed.), ISBN: 978-953-307-419-1, InTech, Available from: http://www.intechopen.com/books/climate-change-geophysical-foundations-and-ecological-effects/climate-change-impacts-on-atmospheric-circulation-and-daily-precipitation-in-the-argentine-pampas-re

INTECH
open science | open minds

InTech Europe
University Campus STeP Ri
Slavka Krautzeka 83/A
51000 Rijeka, Croatia
Phone: +385 (51) 770 447
Fax: +385 (51) 686 166
www.intechopen.com

InTech China
Unit 405, Office Block, Hotel Equatorial Shanghai
No.65, Yan An Road (West), Shanghai, 200040, China
中国上海市延安西路65号上海国际贵都大饭店办公楼405单元
Phone: +86-21-62489820
Fax: +86-21-62489821